Journal of Directed Energy, **4**, Winter 2010, 136–146

Nonintrusive Field Characterization in Interior Cavities with Slab-Coupled Optical Sensor

Bryson Shreeve,* Richard Gibson, Daniel Perry, Richard Selfridge, and Stephen Schultz

Department of Electrical and Computer Engineering, Brigham Young University, Provo, UT 84602

Richard Forber and Wen Wang

IPITEK, Carlsbad, CA 92008

and

Jingdong Luo

University of Washington, Seattle, WA 98195

This paper presents the advances made in electric field sensing using a slab-coupled optical sensor (SCOS). We continue to enhance the use of optical fiber interrogation with electro-optic materials as a method of field sensing. The fabrication materials are all insulators and therefore allow for detection of fields without altering them. The sensors are also much smaller than current metallic field sensors, allowing them to be used in locations in which bulkier sensors cannot be placed. This work uses D-shaped fiber to achieve resonant coupling with electro-optic crystals and polymer. This study reports how a SCOS sensor can perform accurate, low-loss, X-band field detection. We also show how complex fields are analyzed by creating two-dimensional sensors. Each of these advances proves that SCOS devices could be viable solutions for electric field sensing challenges in the area of directed energy weapons.

KEYWORDS: Electric field, Optical fiber, Sensor

Nomenclature

m	slab waveguide mode number
N_f	effective index of the fiber mode
n_o	bulk index of the slab
r_{eff}	electro-optic coefficient, pm/V
t	slab waveguide thickness

Received October 20, 2010.

*Corresponding author; e-mail: brysonshreeve@gmail.com.

$\Delta N/E_{inc}$	figure of merit used in Table 1
ε_r	electrical permittivity
λ_m	wavelength of resonant coupling from fiber to mth slab waveguide mode

1. Introduction

High-power microwave (HPM) weapons are designed to overload and destroy electronic components. One way to protect against such an attack is through shielding. To test the effectiveness of the shielding, one would need to have a compact sensor embedded inside that shielding.

For a sensor to effectively measure the effects of a HPM weapon, it would be best if the sensor itself were nonmetallic and therefore not susceptible to interference from the HPM radiation. A sensor would also need to have high bandwidth for pulsed and high-frequency detection. It would also need to be capable of measuring complex (multidimensional) fields. Furthermore, a sensor in this application (within the shielding) would have to be small and sufficiently sensitive and have optical fiber coupled remote signal processing electronics.

The slab-coupled optical fiber sensor (SCOS) device fulfills all these requirements.[1] First, it consists of solely dielectric materials and is therefore free from the susceptibilities electronics experience. The SCOS has accurately measured fields up to 6 GHz. Complex field measurement is achievable by way of the orientation-specific sensitivity of our devices. The device is also small ($1 \times 0.5 \times 0.2$ mm slab coupled onto an optical fiber) and has sensitivity better than 400 mV/m-Hz$^{1/2}$, and the processing electronics can be fiber coupled a great distance away in shielded areas.

2. SCOS Design

The SCOS consists of an electro-optic slab waveguide coupled to an optical fiber. It functions based on the Pockels effect. The Pockels effect is characterized by an induced change in the birefringence in a material or, in other words, the extraordinary index of refraction changes when an electric field is applied across a sensor.[1]

To get light into the slab waveguide, we rely on evanescent fields. The light launched into the fiber is always vertically polarized, and D-fiber is polarization maintaining. If the slab is close enough to the core of the fiber, a significant amount of light will couple from the core into the slab if there is a mode in the slab waveguide that is phase-matched to the mode in the optical fiber. Figure 1 shows a D-shaped optical fiber in which the optical fiber core is close to the surface. This allows us to use hydrofluoric acid to etch the flat surface so that it is within 500 nm of the fiber core, while still having a fiber width greater than 80 μm.

When the slab is close enough to the core and there is a match between the effective index of the fiber mode and one of the slab modes, a substantial amount of the power will leave the fiber and couple into the slab.[1] The wavelengths at which the slab waveguide modes are resonant with the fiber mode, and therefore couple, are given by Ref. 2:

$$\lambda_m = \frac{2t}{m}\sqrt{n_0^2 - N_f^2},$$

where m is the mode number, t is the thickness of the slab, n_0 is the refractive index of the slab, and N_f is the effective index of the fiber mode. Figure 2 shows that a broadband

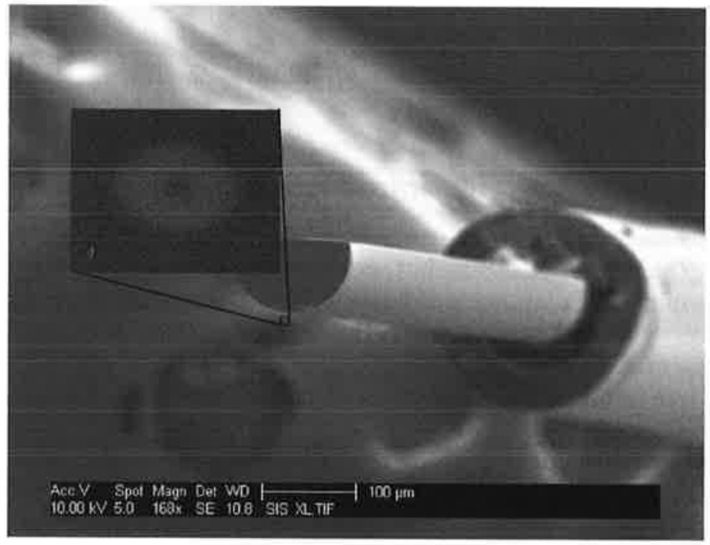

Fig. 1. Scanning electron microscope image of D-shaped optical fiber (125 μm wide).

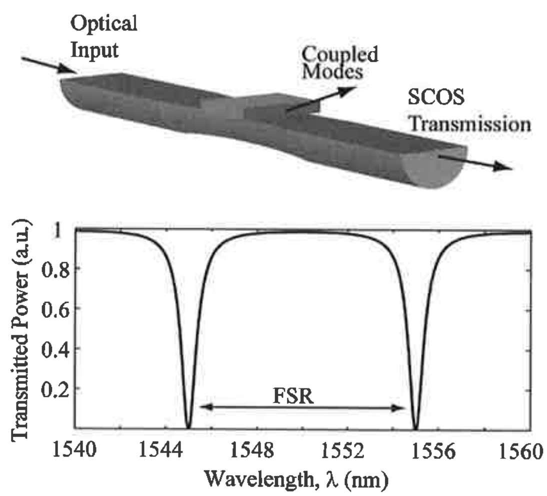

Fig. 2. Characteristic spectrum of light through a SCOS device.

source of light transmitted through a SCOS device has a periodic spectrum where light is lost from the core mode into the slab modes.

Because the resonant wavelength of the mth mode, λ_m, is dependent on the refractive index, the whole transmission spectrum will shift. This shift occurs as the applied electric field causes a change in the index, n_0, of the slab. Figure 3 shows that a small shift in the resonant wavelength causes a large change in power at an operating wavelength at which there is a large slope. When an electric field is applied, a change in power occurs whose relative amplitude is dependent on the strength of the field and whose frequency equals that of the

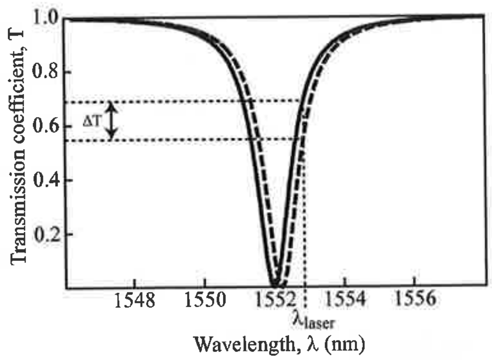

Fig. 3. The transmission spectrum of a SCOS device without (solid) and with (dashed) an applied electric field.

electric field.[1] The signal power (or change in power) is given by the following equation:

$$P_S = P_0\left(\frac{\Delta T}{\Delta\lambda}\right)\left(\frac{\Delta\lambda}{E}\right)E.$$

The signal power is dependent on three factors: the input power (P_0), the slope of the resonance ($\Delta T/\Delta\lambda$), and the spectral shift ($\Delta\lambda/E$) due to the applied field E. The input power is reduced by the fiber splices (especially with the unique D-shaped fiber), but the benefits of D-fiber still make it the fiber of choice. The slope of the resonance ($\Delta T/\Delta\lambda$) depends on the fabrication and is typically measured. The spectral shift ($\Delta\lambda/E$) depends on the materials used and is discussed in the next section.

3. EO Materials

We can enhance the measurement sensitivity by choosing a material that will exhibit a large resonant slope ($\Delta T/\Delta\lambda$) and a large spectral shift ($\Delta\lambda/E$). We have used several inorganic crystal slabs and polymer films as the electro-optic (EO) slab. The sensitivity of the SCOS increases with bulk index of refraction n_0; however, it is more sensitive to the electro-optic coefficient r_{eff} and the electrical permittivity ε_r. Table 1 summarizes these important parameters for various materials amenable to the creation of SCOS devices. This table also includes a figure of merit ($\Delta N/E_{inc}$) that takes into account all of these material parameters. The material that has the highest figure of merit is the EO polymer because it has a large electro-optic coefficient in combination with a low electrical permittivity. Even though the EO polymer has the best theoretical figure of merit, it does not always make the best SCOS because of the difficulty in maintaining a highly parallel slab. A highly parallel slab is necessary because variations in the thickness change affect the slope of the resonance ($\Delta T/\Delta\lambda$). The materials compared are lithium niobate ($LiNbO_3$), lithium tantalate ($LiTaO_3$), potassium titanyl phosphate (KTP), potassium dihydrogen phosphate (KDP), and an EO polymer.

4. Field Characterization

Figure 4 shows that our test setup uses a tunable laser set to the wavelength at which the largest slope occurs. A known field is applied across our SCOS device, and an optical

Table 1. Important properties of EO materials

Crystal	Bulk index, n_o	r_{eff}(pm/V)	ε_r	$\Delta N/E_{\text{inc}}$
$LiNbO_3$	2.18	11	30	7.9
$LiTaO_3$	2.12	10	43	4.5
KTP	1.78	14	13	19
KDP	1.49	10.3	20	2.3
EO polymer	1.75	37	4.0	58

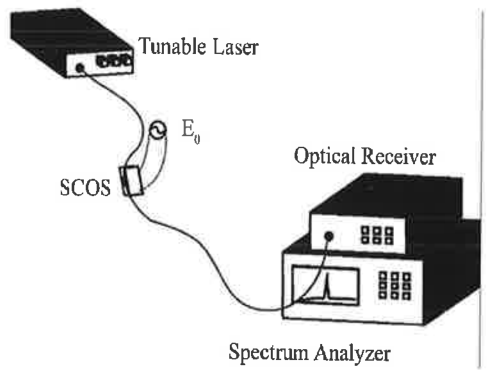

Fig. 4. Signal measurement setup for a SCOS device.

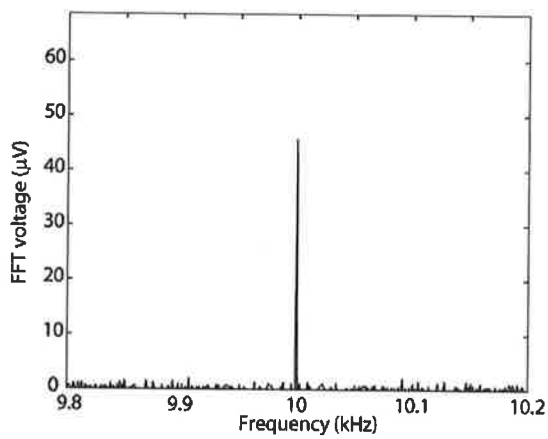

Fig. 5. Spectrum analyzer output has a voltage relative to the field strength.

receiver converts the output signal into an electrical signal, which is input into the spectrum analyzer.

Figure 5 shows a measurement collected by the spectrum analyzer; the large peak corresponds to the frequency of the electric field applied to the SCOS. The voltage peak can now be correlated to the specific known field strength (volts per meter). Once a SCOS device is characterized at several field strengths in this manner, an unknown field can be determined based on the spectrum analyzer output voltage.

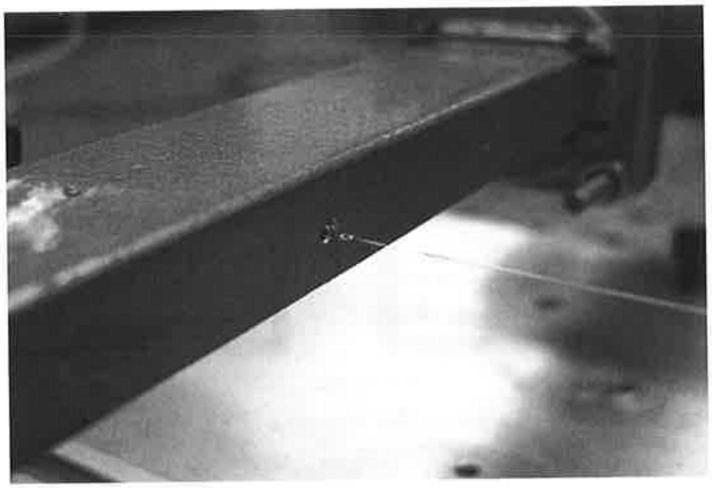

Fig. 6. SCOS device detecting a field inside a waveguide.

Two effects can limit the maximum detectable field: first, if the resonance shifts so much that the laser no long resides on the edge of the transmission resonance. To attain this much shift, the incident electric field would need to be 133 MV/m. The other limiting effect would be damage to the dielectric materials. Based on the materials used, this would require the incident electric field to be less than around 10 MV/m, which is less than the limitation caused by spectral shift. The minimum detectable field is a much more significant limitation and is based on both the electronic noise in the system and SCOS device characteristics. The full characterization of the noise sources was not done for this effort. However, the SCOS devices used in this work were measured to have sensitivity of 400 mV/m-Hz$^{1/2}$.

5. Microwave Field Detection

A SCOS device can be threaded through HPM shielding with entry and exit holes as small as the fiber itself (125 μm). The laser input and optical detector can then be connected from far away with an optical cable. The sensor itself can easily fit inside the shielding as it is generally a $1 \times 0.5 \times 0.2$ mm slab coupled on a 125-μm fiber.

For our SCOS device to sense HPM fields, it must have a high bandwidth. We have tested in fields from 1 kHz to 6 GHz. It is anticipated that it should be able to sense fields much higher, until the wavelength ($\lambda = c/f$) approaches the slab length (1.2 mm). The frequency at which this occurs is $f = c/\lambda = 3.0\,\text{e}8/1.2\text{e}{-3} = 250\,\text{GHz}$. Our high-frequency test (6 GHz) was set up by placing a SCOS inside a waveguide cavity. Figure 6 shows that the test was accomplished by drilling a 1-mm hole through an x-band waveguide and threading the SCOS device through it. By moving the device in small increments, we were able to accurately characterize the field within the waveguide at 6 GHz.

In this test, we excited the TE_{10} mode. We compared the measured field against the expected field (Fig. 7a). We measured with the field normal to the optical fiber (Fig. 7b) by moving the SCOS horizontally through the waveguide at 1-mm increments and measuring each point. We also measured with the field parallel to the optical fiber (Fig. 7c) by moving the SCOS vertically through the waveguide at 0.5-mm increments.

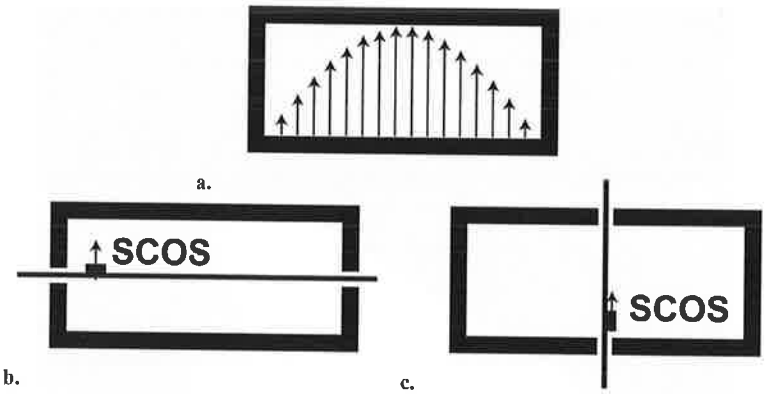

Fig. 7. (a) The TE10 mode of a waveguide. Testing a SCOS (b) perpendicular (c) parallel to the field.

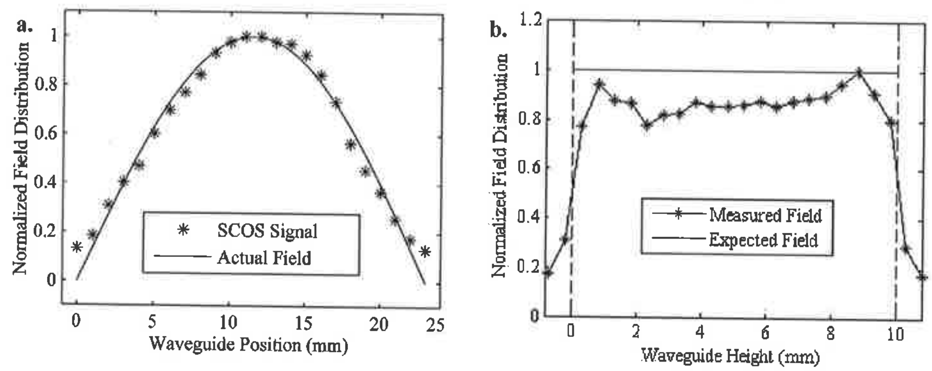

Fig. 8. (a)-Horizontal waveguide characterization. (b)-Vertical waveguide characterization. This measurement varies by up to 20% of the expected value. This is likely due to the holes drilled for insertion of the sensor.

These measurements should work because the optical axis of the slab waveguide is normal to the flat surface of the fiber. It should therefore be sensitive to a field perpendicular to it. The field characterization test in normal orientation can be seen in Fig. 8a. As expected, the SCOS device accurately characterized the TE_{10} mode while the field was perpendicular to the top surface of the slab. The field characterization in parallel orientation (in Fig. 8b) has a constant field distribution across the height of the waveguide as expected.

While in this setup, we also used the waveguide to estimate induced loss. The loss was measured in a hollow core waveguide with nothing inserted, with an optical fiber, and with three different wire widths (10, 50, and 70 μm). Although larger than the wires, the fiber had little significant effect on waveguide transmission, as seen in Table 2. With the waveguide tests mentioned above, we proved that SCOS devices are capable of measuring up to 6-GHz fields, all while having only about a 1% perturbation in waveguide mode.

6. Multiaxis Detection

Owing to the orientation-specific sensitivity of the sensors, The SCOS sensors are able to distinguish complex fields. Figure 9 shows how two dimensionality can be achieved by

Table 2. Measurement of perturbation of fiberoptic cable compared to copper wires

Material	Diameter (μm)	Q	Loss/pass (%)
Air	0	1,696	~1
Fiber	125	1,651	~1
Wire	10	297	7
Wire	50	131	15
Wire	70	75	27

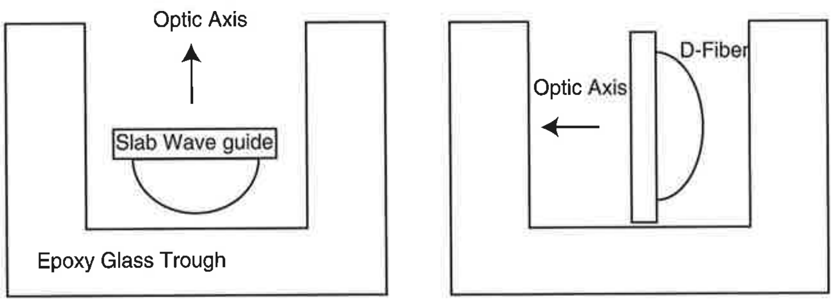

Fig. 9. Two-dimensional SCOS device.

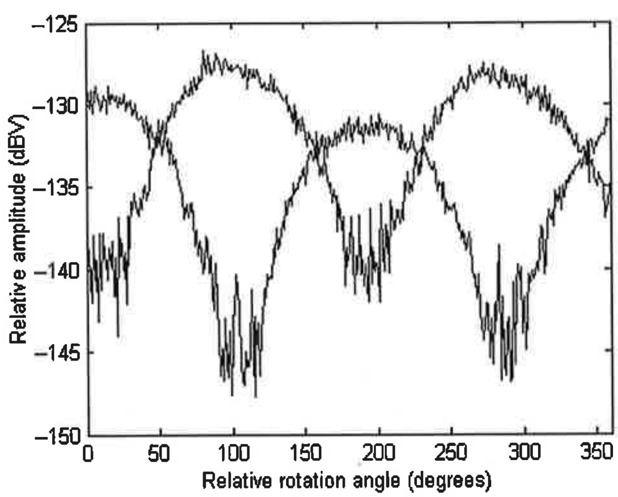

Fig. 10. SCOS rotation. Two sensors perpendicular have peak sensitivity 90 degrees apart.

using two identical SCOS with electro-optic slabs that have optical axes perpendicular to the propagation direction. The two sensors are then attached 90 deg from one another. This method requires that two sources and two detectors be used.

A two-dimensional SCOS was fabricated and tested in a rotation stage. The graph in Figure 10 shows the relative sensitivity of each SCOS as a function of rotation angle. Each SCOS is directionally dependent. They are more sensitive to fields normal to the sensor.

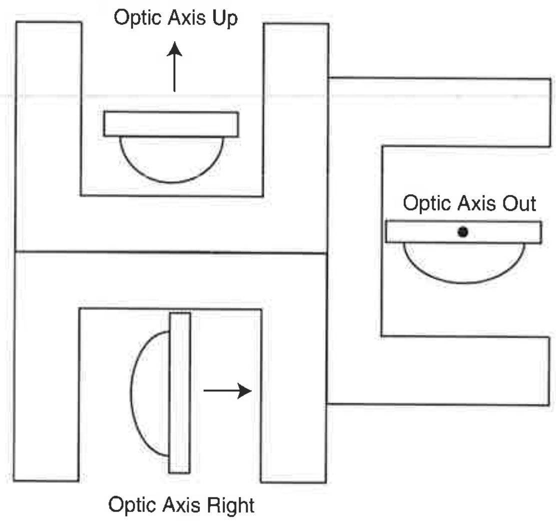

Fig. 11. Three-dimensional SCOS device.

A three-dimensional SCOS was also made using a third sensor whose optic axis is parallel to the length of the fiber. Figure 11 shows how these three SCOS sensors are aligned. Another proposed method of multidimensional sensing is to put multiple crystals on a single fiber. This method will be discussed in future work, along with a more detailed statistical analysis on crosstalk.

7. Conclusion

The SCOS device is a nonintrusive electric field measurement device because it is very compact in size, uses all dielectric materials, and facilitates the separation of detection equipment from the test site. The nonintrusive nature of the SCOS is demonstrated by inserting it into a resonant waveguide and verifying that it does not perturb the waveguide mode. The SCOS is also configured into a three-axis configuration for multidimensional electric field testing.

8. Acknowledgments

The authors gratefully acknowledge the Test Resource Management Center (TRMC) Test and Evaluation Science & Technology (T&E S&T) Program for their support. This work is funded by the T&E S&T Program through the U.S. Army Program Executive Office for Simulation, Training and Instrumentation's contract number W900KK-08-C-0021. We also thank KVH Industries for their donations in conjunction with this research.

References

[1]Gibson, R., *Slab Coupled Optical Fiber Sensors for Electric Field Sensing Applications*, Brigham Young University, Provo, UT (2009).

[2]Kim, K.T., D.S. Yoon, and G.-I. Kwoen, *Opt. Commun.* **230**(1–3), 137 (2004).

The Authors

Dr. Richard Forber received his Ph.D. in physics from the Massachusetts Institute of Technology in 1983. He has accumulated more than 27 years of experience leading and managing industrial R&D technology programs. During 20 years at HRL Laboratories in Malibu, California, Dr. Forber developed a wide range of technologies including fiber and integrated optics, liquid crystal spatial light modulators, infrared and visible image projection systems, and high-power phase conjugate lasers. Dr. Forber joined IPITEK in Carlsbad, California, in 2004 as Senior Research Scientist and Manager of the Defense, Aerospace, and Avionics R&D Group. He provides technology and management leadership over numerous DoD contracts and internal R&D, he is the principal lead for DoD business development, and he actively participates in research of polymer photonics, fiber-optic photonic links, and fiber-optic sensors. Prior to IPITEK, Dr. Forber was Program Manager and Sr. Research Director at JMAR Technologies, San Diego, leading development and marketing of high-power laser plasma x-ray sources, x-ray optics, and x-ray lithography systems. Dr. Forber has more than 50 technical publications and numerous conference presentations in a wide variety of technology areas.

Dr. Richard Gibson received his Ph.D. in electrical engineering in 2009 at Brigham Young University, where he spent 4 years researching fiber-optics–based electric field sensors. He was a 2009 recipient of the DEPS fellowship for his research on electric-field characterization with optical fiber sensor arrays. Richard currently works at Harris Corporation in Melbourne, Florida.

Dr. Jingdong Luo is currently a Senior Research Scientist at the University of Washington. He is involved in research with the Materials Science and Engineering Department and leads a group in Organic Photonics.

Mr. Daniel Perry is currently studying electrical engineering at Brigham Young University. There he joined the electro-optics lab in April 2009 and has been researching fiber-based optical sensors. In winter 2011 he will graduate with a B.S.E.E. and hopes to continue on to graduate school.

Dr. Stephen M. Schultz received B.S. and M.S. degrees in electrical engineering from Brigham Young University in 1992 and 1994, respectively. He received a Ph.D. in electrical engineering from the Georgia Institute of Technology, Atlanta, Georgia, in 1999. He worked at Raytheon Missile Systems from 1999 to 2001. He has taught at Brigham Young University since 2002 and is currently an Associate Professor. He has authored or coauthored more than 70 publications and holds 10 patents. His research interests are in the area of optical fiber devices with an emphasis on optical fiber–based sensors.

Dr. Richard Selfridge joined the ECEn Department at Brigham Young University in 1987. He received his Ph.D. in electrical engineering from the University of California, Davis, in 1984. His research has focused on in-fiber optical devices including fiber Bragg gratings (FBGs), modulators, and sensors. In addition, he has collaborated with other researcher in programs to develop new techniques for demodulating optical signals from FBGs that retain not only peak data but display the entire substructure of the FBG response. He teaches courses in optical engineering, electronics, and solid-state devices. His research efforts have been funded by the NSF, organizations within the DoD, and a few private companies including IPITEK and KVHI.

Mr. Bryson Shreeve is a master's student in electrical engineering at Brigham Young University. Bryson received his B.S. in electrical engineering from Brigham Young University in 2009. He has been involved in research in fiber-optic–based electric and magnetic field sensors as an undergraduate and graduate student. In his research, he has pioneered the magneto-optic slab coupled optical sensor.

Dr. Wen C. Wang received his B.S. and M.S. degrees in physics from National Tsing Hua University, Hsinchu, Taiwan, in 1973 and 1977, respectively, and his Ph,D, degree in physics from the University of Southern California in 1982. After 1 year of postdoc at USC, he joined San Diego State University as research faculty until 1988. From 1988 to 2000 he was a senior optical engineer at Anacomp, Inc., San Diego. In 2000 he joined IPITEK, Inc., as a staff scientist, where he is developing optical fiber sensors, which include vibration, stress, chemical, E-field, and B-field sensors, as well as super wideband optical antennas and RF over fiber with high spurious free dynamic range.